ORIGINAL PAPER

Mechanical characteristics and freeze–thaw damage mechanisms of mode-I cracked sandstone from the Three Gorges Reservoir region under different chemical solutions

Tielin Han[1,2,3] · Zhihui Li[2] · Junping Shi[1] · Xiaoshan Cao[1]

Abstract

In consideration of the actual environment of the cold region, a test scheme of freeze–thaw (FT) cycles was adopted to explore the mechanical characteristics of sandstone with mode-I cracks under the three-point bending, tensile, and compressive compression tests. And to explore the chemical and freeze–thaw (FT) damage mechanisms, variations in the ion concentration of solutions and the microstructures of sandstone are observed and analyzed under the FT cycle. Experimental results show that the sandstone has a marked tendency to weaken after repeated FT cycles. The pH and chemical composition of chemical solutions had different effects on the deterioration degree from FT in sandstone. From the combined effects of the chemical corrosion and the FT cycles, the ion concentration that was dissolved from a chemical solution had a clear, cumulative time periodicity. The surface of the sandstone sample was found to exhibit variable degrees of degradation after the combined effects of chemical solutions and FT cycles, and with an increasing number of FT cycles, the degradation degree in the surface microstructure of the sandstone gradually increased. Meanwhile, the interior of sandstone samples was clearly degraded. Specifically, the size of mineral particles was reduced, their edges and corners gradually disappeared or became smooth, the surface roughness of the mineral was found to decrease, and its structure became loose.

Keywords Chemical erosion · FT cycle · Coupling effect · Sandstone · Damage degradation · Mesoscopic mechanism

✉ Tielin Han
s3050210133@163.com

Zhihui Li
lizhihui@xaut.edu.cn

Junping Shi
shijp@xaut.edu.cn

Xiaoshan Cao
caoxsh@xaut.edu.cn

1 State Key Laboratory Base of Eco-Hydraulic Engineering in Arid Area, Xi'an University of Technology, Xi'an, Shaanxi 710048, People's Republic of China

2 School of Mechanical Engineering, Baoji University of Arts and Sciences, Shaanxi 721016, People's Republic of China

3 Guangdong Provincial Key Laboratory of Durability for Marine Civil Engineering, College of Civil Engineering, Shenzhen University, Shenzhen, Guangdong 518060, People's Republic of China

Introduction

For a long time, researchers had considered the effect of water on the mechanics of rocks solely from the effective stress principle of Terzaghi (1943), ignoring the complex stress corrosion that occurs during water–rock interaction. With the increasing number of studies on water–rock interaction and the research intersection of multiple disciplines in recent years, researchers have gradually come to realize that it is also necessary to consider the complex stress corrosion that may occur in water–rock and not just focus on the chemical interactions that can be observed between water and rock.

Much of the research in the field has been conducted by Chinese and international scholars, and many useful results have been obtained. Lajtai et al. (1987) investigated the effect of moisture on the deformation and strength of rock, and they also studied the influence of water on the uniaxial compression strength and modulus elasticity of rocks. Atkinson and Meredith (1981) found that the chemical composition and flow of chemical solutions indeed have a marked effect on the crack propagation rate of quartz.

Karfakis and Askram (1993) conducted a study on the fracture toughness of rock when exposed to different chemical solutions. Dunning et al. (1994) found that fracture toughness of rock in a dry environment is greater than that in a humid environment but that the crack propagation rate is reduced in a dry environment. Han et al. (2019) found that the interaction of water and rock has a greater effect when a solution reaction occurs under exposure to acidic solutions but that the dissolution of rock in salt solutions is consistent with physical dissolution. Li et al. (2018) established a chemical damage strength model based on the corrosion effects on calcareous cement and sandstone under variable acidic chemical solutions. Jia et al. (2017) proposed an elastic-plastic model taking into account plastic shearing and pore collapse for the cement paste. Feng and Ding (2007) and Zhang et al. (2019) carried out a systematic experimental study on the mechanical properties of rock in different chemical solutions, and based on the observed chemical damage and the CT number, a new damage variable was defined. And they also examined the entire process of destroying cracked rocks submerged in variable chemical solutions using a homemade mesoscopic loading test instrument (Feng and Ding 2007; Zhang et al. 2019).

Bäckström et al. (2008) quantitatively modeled the uniaxial compressive failure of granite both with and without saline porewater. Négrel et al. (2010) focused on the composition of granitic parent rock and water chemistry by measuring lead isotopes in water using a multicollector inductively coupled plasma mass spectrometer. Zhou et al. (2018) systematically studied the effect of water-chemical dissolution on the morphology of rock surface. Wu (2013) investigated the time-dependent characteristics of sandstone under chemical corrosion. Important studies were carried out on the strength of prefabricated cracks in sandstone samples and the friction coefficient in the sample surface when submerged in water-chemical solutions (Feucht and Logan 1990; Dieterich and Conrad 1984). Other researchers tested and measured the influence chemical solutions have on fracture toughness in rocks (Nara et al. 2012; Reinhardt et al. 2014). Zeng et al. (2015) proposed a polycrystalline model to study the elastic-plastic behavior of sandstone. Taken as a whole, the aforementioned research findings provide the foundation for studying the fracture mechanics of rock submerged in water-chemical solutions. However, it must be noted that most of the aforementioned test schemes were adopted to saturated rock and rock soaked in a chemical solution and did not take into account the effects that occur in an actual rock mass environment. Therefore, it is necessary to consider the practice of rock engineering when experimentally studying the effects of water on fracture toughness in rocks.

Rock engineering, for example, the engineering conducted on the bank slopes of reservoirs, is most often applied in a complicated environment that is often subjected to adverse weathering. Weathering often contributes to the deterioration of the mechanical characteristics in rock, which can seriously affect the service life of a rock mass that is utilized in an engineering project. Temperature change is one of the main factors in weathering. Due to the diurnal or seasonal variation in temperatures, rock often suffers from the effects of the freeze–thaw (FT) cycle, which leads to variable degrees of degradation and damage in rock, especially in cold areas.

Fukuda (1974) describes the primary factors that affect the FT strength of rocks, such as the rock type (lithology), temperature, moisture state, and duration of FT cycles. McGreevy (1985) points out that the moisture content of rock has a great influence on the degree of FT damage it accumulates. Inada and Yokota (1984) found that regardless of whether the rock is saturated or dry, its compressive and tensile strength increases with a decrease in temperature, primarily due to mineral contraction and the strength of frozen water. Aoki et al. (1990) found that rock porosity increases with a greater number of FT cycles but that the longitudinal wave velocity and tensile strength of rock were reduced by approximately 10 to 20% at the same time. Hallet (1983) found that water migration in tuff has a serious influence on FT damage in rock but that this is rarely the case for shale and andesite. Norikazu (1990) and DelRoa et al. (2005) utilized the observed degradation degree in longitudinal wave velocity to indirectly determine the degree of FT damage that occurs in the microstructure of rock during the FT cycle. Chen et al. (2010) tested the effects FT cycles have on the different moisture states of Japanese tuff samples taken from Sapporo. Fang et al. (2019) established the damage statistical constitutive model of loaded rock and the method for determining its parameters under freeze–thaw conditions. Yamabe and Neaupane (2001) conducted an experimental study on the effects that FT cycle thermal expansion and uniaxial compression under different temperatures. Yavuz et al. (2006) tested the effects the FT cycle has on different types of rocks at variable temperatures. Tan et al. (2011) conducted an experimental study on the compressive strength of granite samples before and after FT cycles at temperatures from −40 to 40°C. Fang et al. (2014) carried out indoor FT cycle tests on sandstone samples taken from the Yungang grottoes. Chen et al. (2014) systematically studied the effect FT cycles have on the mechanical properties of granite and discussed its damage mechanisms. Cao et al. (2020) studied the effects of freezing temperature and the number of freeze–thaw cycles on the fracture characteristics of sandstone under different fracture modes (Koorosh et al. 2020).

In summary, the research results mentioned previously function as a foundation for studying the mechanics of intact rock under FT cycle exposure. However, it must be noted that the aforementioned tests were not specifically related to the effect FT cycles have on the fracture toughness of rock. Experimental testing has found that rock failure is closely related to the fractures rock will accumulate. Many scholars

have used the fracture toughness of rock to evaluate the safety and stability of rock used in engineering projects quantitatively. With this in mind, we can see that the study of the effects that FT cycles can have on the fracture toughness of rock is of great importance. In addition, rock engineering is undertaken in a complicated environment, and rocks are oftentimes simultaneously subjected to exposure from chemical corrosion and FT cycles. Therefore, it is necessary to study the effects that different chemical solutions will have on a rock that is subjected to repeated FT cycle exposure, especially when it comes to prefabricated cracked rock.

In consideration of the actual environment of the hydrofluctuation belt of a typical bank slope, a test scheme for rapid FT cycle exposure is adopted to explore the physical and mechanical characteristics of sandstone with mode-I crack. The fracture toughness (i.e., K_{IC}) testing, tensile strength testing, and compressive strength testing on mode-I cracked sandstone are conducted under the combined effects of chemical corrosion and FT cycles. The damage mechanisms of chemical-FT damage are analyzed and studied from the microperspective by means of microdetection methodology.

Tests and methods

Sample preparation

Sandstone samples extracted from a typical bank slope in the Three Gorges Reservoir region of the Yangtze River in China were used in this study's tests. The location map of the Three Gorges Reservoir is shown in Fig. 1. Specifically, the type of rock was calcareous quartz sandstone characterized by a high degree of homogeneity and integrity (as shown in Fig. 2).

Strictly according to accepted guidelines (China 2007) using a three-point bending method, we measured the fracture toughness (K_{IC}) of straight-incision cuboid sandstone with mode-I fractures. The depth of the straight incision was 21 to 23 mm, and its width was 1.0 mm; the cross-sections were square with an area of 50×50 mm^2 and a height of 250 to 260 mm.

The computational formula of fracture toughness K_{IC} (in MPa·m$^{1/2}$) can be expressed as follows:

$$K_{IC} = 0.25 \frac{S_d P_{\max}}{B\ B^{1.5}} y\left(\frac{a}{B}\right) \tag{1}$$

$$y\left(\frac{a}{B}\right) = \frac{12.75 \left(\frac{a}{B}\right)^{0.5} \left[1 + 19.65\left(\frac{a}{B}\right)^{4.5}\right]^{0.5}}{\left(1 - \frac{a}{B}\right)^{0.25}} \tag{2}$$

where B denotes the specimen width (cm), which is equal to the specimen height W (cm); S_d represents the distance between two supporting points (cm); $P_{\max}$ denotes the load leading to the fracture failure (N); a is the depth of straight incision (cm).

In the experiments, 276 sandstone samples were selected and divided into 21 groups. One group was used to measure fracture toughness K_{IC}, uniaxial compression strength, and tensile strength of natural sandstone samples. The remaining sandstone samples were used to experimentally study the effects of the FT cycles and different chemical solutions.

Preparation of chemical solutions

Existing research shows that rock-mass engineering projects in reservoir dams, coastal areas, and inland saline lakes are often subjected to sulfate erosion, and acid rain exists mainly in the form of sulfate in China. In rock-mass engineering projects in the Three Gorges Reservoir region in China, the main ion composition of reservoir water is OH$^-$, SO$_4^{2-}$, Cl$^-$, Na$^+$, K$^+$, HCO$_3^-$, and so forth; and the pH range of the reservoir water is 6.35 to 8.03. In addition, damage to the rock mass, which generates and accumulates until destruction, is a long and slow process. To observe these changes in a relatively short time, we chose lower or higher pH values of chemical solutions to carry out the research. Consequently, we chose sodium sulfate (Na$_2$SO$_4$), NaOH, and NaHCO$_3$ solutions as corrosion compounds (as shown in Table 1). Each chemical solution was reconfigured every 25 FT cycles to maintain its initial concentration and pH.

Test apparatus and test method

In winter, the temperature in the Three Gorges Reservoir region of China ranges from a low of −15°C to a high of 9°C with an average temperature of −3°C. Therefore, the authors used temperatures from −20 to 20°C. CABR-HDK9A model rapid FT testing machine was used for this study, and each FT cycle was calibrated to last approximately 4 h.

Before commencing testing, the sandstone samples were dried at 105°C for 48 h to maintain a constant weight and were subsequently cooled for mass measuring. Later, a vacuumization method was utilized to seal the dried samples in the chemical solutions, presented in Table 1, until saturation. Specifically, the volume of all chemical solutions used for soaking was 0.6 L. Thereafter, the chemical solutions and the samples were placed in the FT testing machine to begin FT tests. The experiment was carried out in a closed environment to prevent water from evaporating. The sandstone samples were taken out every 25 cycles to carry out the corresponding experimentation and observation. Four tests were conducted in parallel for each chemical solution under each test cycle. To further explore the variation regularity of tests, physical and mechanical parameters of sandstone samples were tested in saturation.

Fig. 1 Location map of the Three Gorges Reservoir

The study's mechanical tests were conducted using a WDT-1500 large-scale multifunctional reactive material testing machine. Displacement loading was adopted for the entire process of testing, and the tests were performed according to the accepted guidelines (China, 2007). An XTL-100E binocular microscope and scanning electron microscopy (SEM) and energy dispersion spectrum (EDS) machines were used to observe the surface of the rocks and their internal microstructures. In addition, ion dissolution in the study's chemical solutions was measured using a TAS-990 atomic absorption spectrophotometer.

Test result and analysis

Analysis of mechanical characteristics

The fracture toughness (K_{IC}), tensile strength, and uniaxial compressive strength of sandstone samples, as exposed to the combined effects of chemical corrosion and FT cycles, are presented in Fig. 3. From the results presented, it can be seen that fracture toughness (K_{IC}), tensile strength, and uniaxial compressive strength all tend to be markedly weaker following the samples' exposure to FT cycles in different

Fig. 2 Microscope images of sandstone: (**a**) white mica cementation and (**b**) potassium feldspar angular debris

(a)
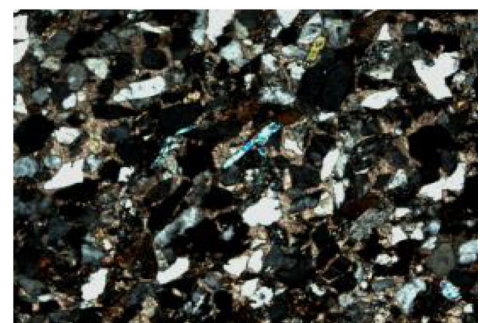
(b)

Table 1 Preparation of chemical solutions

Chemical xcomposition	Concentration (mol/L)	pH
Na_2SO_4	0.1	3.0
NaOH	0.1	12.0
$NaHCO_3$	0.1	3.0
Distilled water	—	7.0

chemical solutions and gradually accelerated as the number of FT cycles increased.

During the initial 25 FT cycles, the degree of damage to the mechanical properties of the samples was found to be highest in 0.1 mol/L Na_2SO_4 (pH = 3.0) solution and lowest in the 0.1 mol/L NaOH (pH = 12.0) solution. However, when the number of FT cycles exceeded 25, the degree of damage exhibited on the mechanical properties of the sample rock increased in the 0.1 mol/L NaOH (pH = 12.0) solution, was found to be the lowest in distilled water (pH = 7.0), and was found to be

highest in 0.1 mol/L Na_2SO_4 (pH = 3.0) solution. When other conditions remain unchanged, the damage degree to the mechanical properties of samples was higher in the 0.1 mol/L Na_2SO_4 (pH = 3.0) solution than it was in the 0.1 mol/L $NaHCO_3$ (pH = 3.0) solution. The damage was found to be lower in the distilled water (pH = 7.0) than in the 0.1 mol/L Na_2SO_4 (pH = 7.0) solution.

Variation regularity in the ion concentration of chemical solutions

To a certain extent, the concentration of dissolved ions in chemical solutions reflects the degree to which the sandstone samples were damaged under the coupled effects of chemical corrosion and FT cycle. In order to prevent water evaporation, the whole experiment was carried out in a closed environment.

The Ca^{2+}, Mg^{2+}, and Fe (Fe^{3+} + Fe^{2+}) ion concentrations in chemical solutions were measured every 25 FT cycles. The observed relationships between the different ion
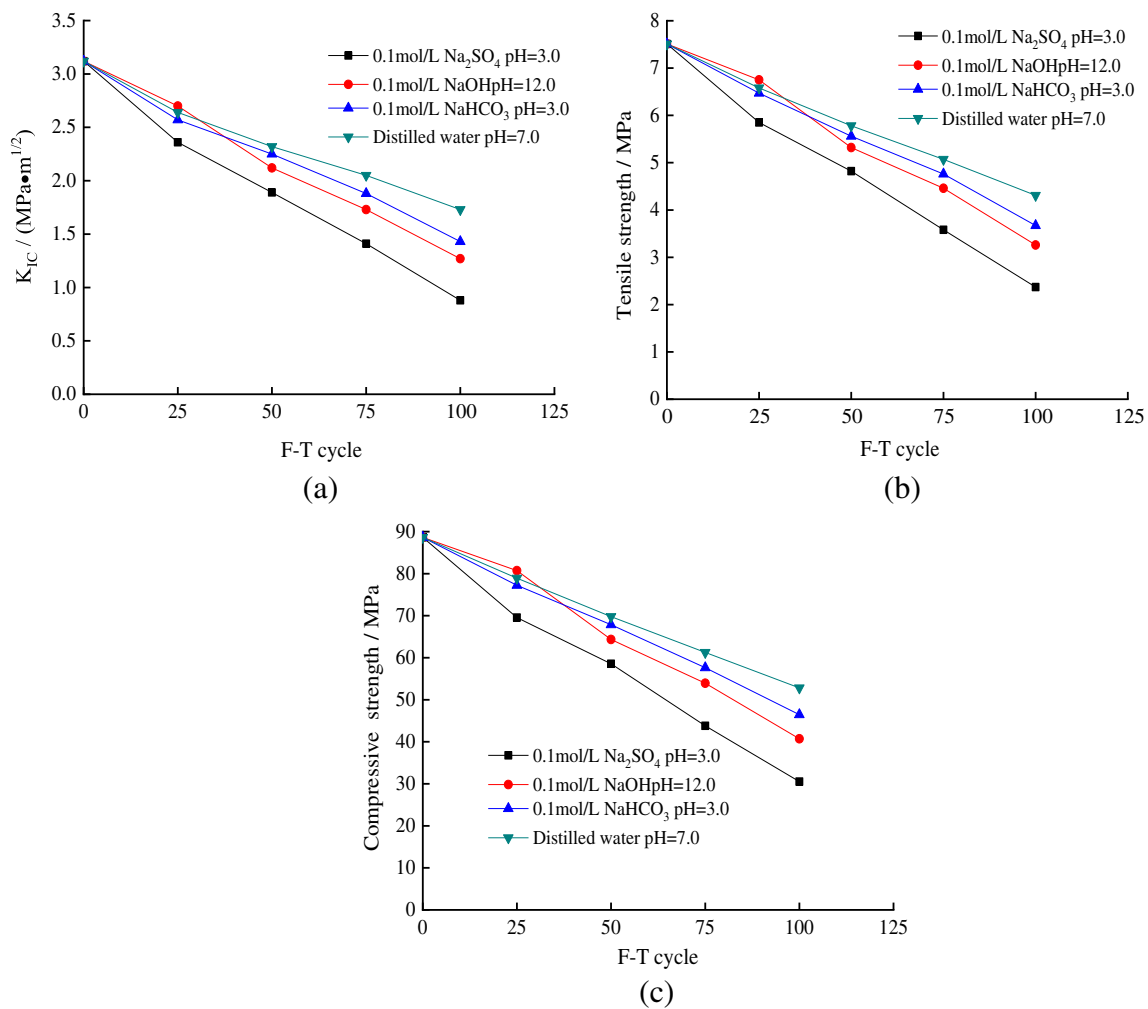

Fig. 3 The relationship among fracture toughness K_{Ic}, uniaxial compressive strength, and tensile strength of sandstone and FT cycles under different chemical solutions

concentrations and the FT cycles under the combined effects of different chemical solutions and FT cycle are presented in Fig. 4.

The results indicated that the pattern of change in the Ca^{2+}, Mg^{2+}, and Fe ($Fe^{3+} + Fe^{2+}$) ion concentration of chemical solutions varied in the same manner as with FT cycles when the specimens were under the combined effects of the chemical solutions and FT cycles. The ion concentrations increased gradually as the number of FT cycles increased under different chemical solutions. This finding indicated that the concentration of dissolved ions in chemical solutions has obvious periodic and cumulative time limits. However, it must be noted that the ion concentrations in solutions were found to increase by varying degrees under continued FT cycle exposure.

The influence of the chemical solution pH

During the initial 25 FT cycles, the concentration of dissolved ions was found to be highest in the 0.1 mol/L Na_2SO_4 (pH = 3.0) solution, in between in the neutral 0.1 mol/L Na_2SO_4 (pH = 7.0) solutions, and lowest in the 0.1 mol/L NaOH (pH = 12.0) solution (as shown in Fig. 4). This is mainly due to a lot of white precipitates (main ingredients were Ca (OH)$_2$ and Mg (OH)$_2$) deposited on the sandstone's surface, which hindered

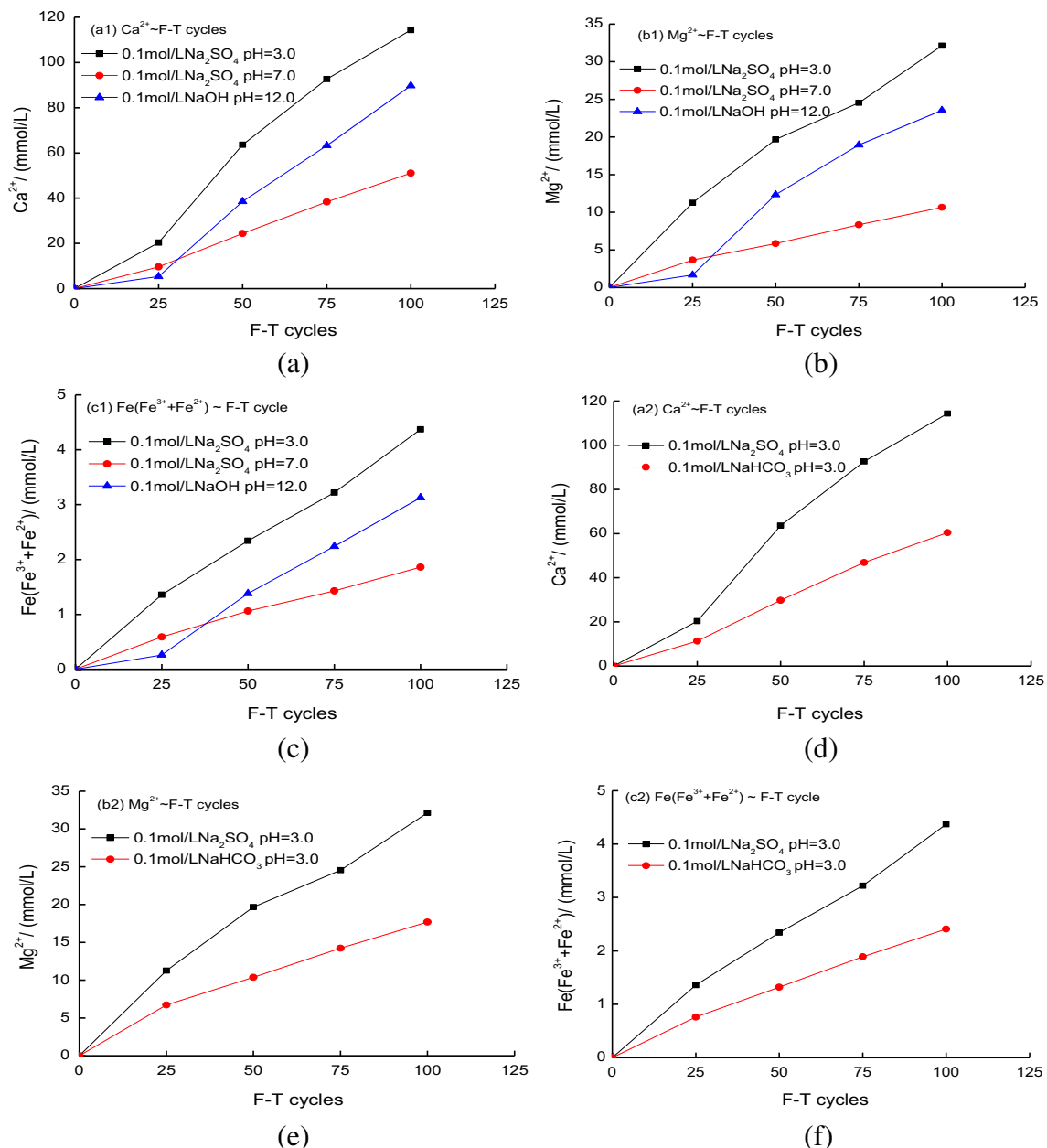**Fig. 4** Curves of Ca^{2+}, Mg^{2+}, and Fe ($Fe^{3+} + Fe^{2+}$) ion concentration and FT cycles under different chemical solutions

chemical solutions to percolate through internal of sandstones and played an inhibition effect on the FT cycles and chemical damage (shown in Fig. 5). Later, white precipitation gradually disappeared when increasing the number of FT cycles, and the concentration of dissolved ions increased in the 0.1mol/L NaOH (pH = 12.0) solution, and the concentrations were variable under variations in the acidity and alkalinity of the chemical solutions. The lowest ion concentration was exhibited in distilled water (pH = 7.0), while the highest ion concentration was exhibited in the 0.1 mol/L Na_2SO_4 (pH = 3.0) solution.

This indicated that the acidic 0.1 mol/L Na_2SO_4 (pH = 3.0) solutions can increase FT damage and deterioration in sandstones. However, a certain inhibiting effect was observed on the deterioration of the study samples soaked in the 0.1 mol/L NaOH (pH = 12.0) solution at the initial stages of testing. The inhibiting effects presented in the NaOH (pH = 12.0) solution gradually decreased and finally disappeared as increasing numbers of FT cycle exposure. This situation was similar for the effects of chemical corrosion and FT cycles on the physical characteristics of sandstone samples, proving further that 25 FT cycles represent a threshold value for the chemical and FT cycle damage absorbed in sandstones that were soaked in the NaOH (pH = 12.0) solution.

The influence of the chemical solutions' chemical components

During the FT cycles, the concentration of dissolved ions was found to be different under the variable chemical compositions of the chemical solutions (as shown in Fig. 4). When the concentration and pH of chemical solutions remained unchanged, the Ca^{2+}, Mg^{2+}, and Fe (Fe^{3+} + Fe^{2+}) ion concentration in the 0.1 mol/L Na_2SO_4 (pH = 3.0) solution was found to be greater than that in the 0.1 mol/L $NaHCO_3$ (pH = 3.0) solution. This indicated that the effect of Na_2SO_4 (pH = 3.0) solution on FT damage was greater than that in an $NaHCO_3$ (pH = 3.0) solution. Moreover, these findings indicated that Na_2SO_4 solutions have a strong influence on FT damage in sandstone due to their concentration of dissolved ions.

Fig. 5 Surface microstructure of sandstone under the combined effect of chemical corrosion and FT cycles
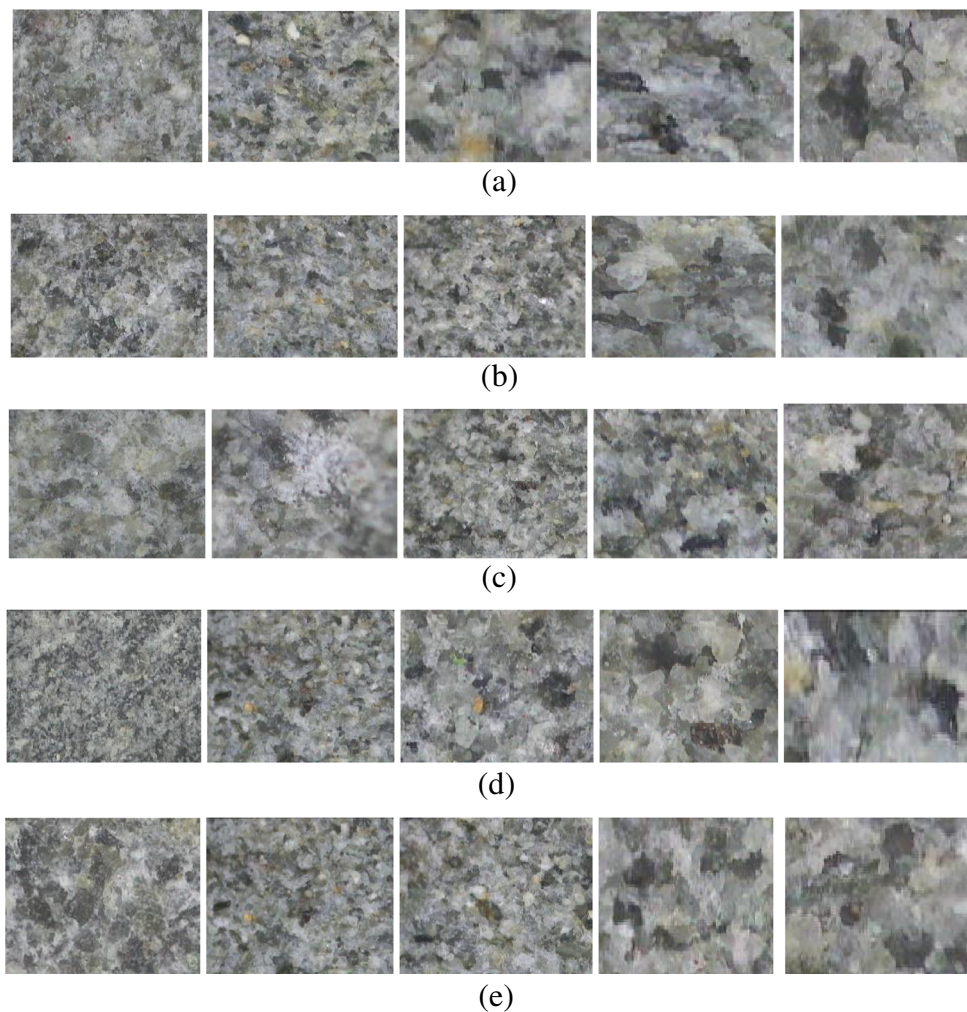
The effect of chemical-FT deterioration of the microstructure of rock

Microstructure characteristics of a rock's surface

To further reveal the damage and degradation mechanisms in sandstone under the combined effects of different chemical solutions and FT cycles, an XTL-100E binocular microscope was utilized to observe the surface microstructure of sandstone samples. In order to remove the possible errors caused by rock inhomogeneity and to ensure the comparability of test results, the same sandstone samples were used for the surface observations, and the image was taken from the same location (as shown in Fig. 5).

As seen in Fig. 5, the surface view is magnified 31 times, showing the observable relationship between surface microstructure and the number of FT cycles undergone in conjunction with the combined effects of different chemical solutions.

The observations indicated that the surface of sandstone became seriously degraded under the combined effects of chemical corrosion and FT cycles (e.g., holes and pitting corrosion will form). The size of the holes and degree of pitting corrosion in sandstone's surface gradually increased with an increasing number of FT cycles. Therefore, it can be concluded that the damage degree of the surface microstructure of sandstone gradually increased over greater amounts of exposure. In addition, it was found that the degree of damage differed when sandstone was immersed in different chemical solutions.

As indicated from Fig. 5, the surface of sandstone soaked in 0.1 mol/L Na_2SO_4 (pH = 7.0) solution or 0.1 mol/L Na_2SO_4 (pH = 3.0) solution exhibited pitting corrosion. Specifically, the greater the number of FT cycles, the greater the size of the holes and the deeper the pitting. The degree of FT damage in the 0.1 mol/L Na_2SO_4 (pH = 3.0) solution was greater than that in the neutral 0.1 mol/L Na_2SO_4 (pH = 7.0) solution. However, it must be noted that the microstructures on the surface of the samples soaked in the 0.1 mol/L NaOH (pH = 12.0) solution were found to have exhibit obvious change after 25 FT cycles.

During this testing, many white precipitates were deposited on the surfaces of the samples. These precipitates were specifically composed of Ca $(OH)_2$ and Mg $(OH)_2$, which hindered the percolation of the chemical solutions through the interior of the sandstone, thereby inhibiting chemical-FT cycle damage. However, these white precipitates gradually disappear until reaching approximately 50 FT cycles, and the size of holes and degree of pitting corrosion on the sample surfaces gradually increased. The hole size and the degree of pitting corrosion were all greater when the sandstones were soaked in the Na_2SO_4 (pH = 3.0), Na_2SO_4 (pH = 7.0), and NaOH (pH = 12.0) solutions after 100 FT cycles.

In addition, the effect of the Na_2SO_4 (pH = 3.0) solution on the damage degree to the sandstone surface was greater than that for the Na_2SO_4 (pH = 7.0) and NaOH (pH = 12.0) solutions. For the NaOH (pH = 12.0) solution, the damage was found to be less than that for the Na_2SO_4 (pH = 7.0) solution during initial testing. However, the damage incurred upon the sandstone soaked in the NaOH (pH = 12.0) solution gradually increased with the increasing number of FT cycles. This further indicated that Na_2SO_4 (pH = 3.0) aggravated FT damage of the samples. However, the caveat here that during initial testing was a certain inhibiting effect on FT damage in the samples soaked in NaOH (pH = 12.0) solutions as the number of FT cycles increased. This inhibiting effect in the NaOH (pH = 12.0) solution was found to gradually disappear after more than 25 FT cycles.

As shown in Fig. 5, different chemical compositions exhibit variable effects on the microstructure of sandstone. When other conditions were static, the effect of the Na_2SO_4 (pH = 3.0) solution on the size of the holes and degree of pitting corrosion in the sandstone's surface was found to be greater than that for the $NaHCO_3$ (pH = 3.0) solution. A discreet influence was observed from the neutral solutions on the damage deterioration in the rock's microstructure. The effect of the Na_2SO_4 (pH = 7.0) solution on the size of the holes and the degree of pitting corrosion in the sandstone surface was greater than that for distilled water (pH = 7.0). These last two findings are presented in Fig. 5b and Fig. 5e, respectively. These findings signify that Na_2SO_4 solutions will aggravate FT damage in sandstone.

SEM and EDS observations of the internal microstructure of the samples

To further reveal the mechanisms of damage degradation in sandstone under the combined effects of various chemical solutions and FT cycles, SEM and EDS machines were used to observe the internal microstructure of the samples. Figure 6 shows the SEM results for the internal microstructures of the sandstone samples after exposure to 100 FT cycles under the combined effects of different chemical solutions and FT cycles. The EDS testing examined small areas of the sandstone samples, which were found to have a variety of minerals distributed haphazardly inside the rock. Thus, the results of the EDS testing presented in this study are the average of the test results.

As shown in Fig. 6, corrosion degradation in the sandstone interior was observed to varying degrees in samples undergoing the combined effects of chemical corrosion and FT cycle exposure. The internal morphology of the sandstone samples was found to be relatively coarse in its natural state. Using the EDS, it was found that the samples were composed primarily of SiO_2, the size of the samples' mineral particles was relatively large, the edges and corners of the mineral grains were

Fig. 6 SEM images of sandstone under different chemical solutions after 100 FT cycles

(a)   (b)   (c)

(d)   (e)
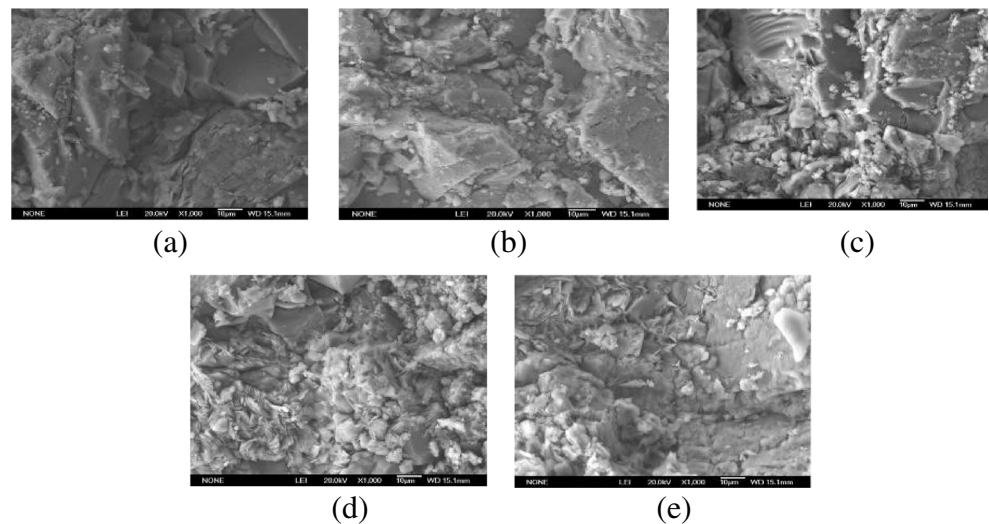
very clear, and the sandstone samples' structure was dense. However, many small mineral particles formed in the internal microstructure of the rock under the combined effects of different chemical solutions and FT cycle exposure. Moreover, the edges and corners of the mineral grains gradually disappeared or became smoother. In addition, the roughness of the mineral grains gradually decreased, eliciting a looser structure.

The results presented in Fig. 6 indicate the extent to which FT damage and degradation in indented sandstone differed when immersed in variable chemical solutions. It was found that the sensitivity of sandstone to different chemical solutions was varied. When other conditions remain unchanged, the damage and degradation in sandstones accrued from FT cycle exposure were controlled by the sample's chemical environment.

As shown in Figs. 6, 7, 8, 9, 10, and 11, the size of mineral particles in indented rock decreased when the samples were immersed in the Na_2SO_4 (pH = 3.0) solution after 100 FT cycles. The degree of surface coarseness steadily reduced, while the grinding and roundness of the mineral grains increased from gradual corrosion. Meanwhile, due to corrosion in the cement between mineral grains composed primarily of

$CaCO_3$, the structure of the indented sandstone samples became looser. These findings were consistent with the results of the study's EDS testing as well. Relative to the natural state of sandstone, the mineral particle sizes, grinding, and roundness of mineral grains decreased to variable extents when immersed in Na_2SO_4 (pH = 7.0) and NaOH (pH = 12.0) solutions but were still greater than in Na_2SO_4 (pH = 3.0) solution.

After conducting a comparative analysis, it was found that the particle size, grinding, and roundness of the mineral grains of samples in the Na_2SO_4 (pH = 7.0) solution were greater than those in the NaOH (pH = 12.0) solution. However, it must be noted that the degree of mineral particle coarseness and the looseness of the internal structure in sandstone were smaller than that in the NaOH (pH = 12.0) solution. The calcareous cement of sandstone samples submerged in the Na_2SO_4 (pH = 3.0) solution was completely corroded. Moreover, the results of EDS testing showed that all Ca^{2+} elements were no longer present and that the number of other elements also decreased relative to what was typically found in the samples' natural state. The sandstone sample elements in the NaOH (pH = 12.0) solution had been reduced relative to the sample's natural state. However, some elements did not
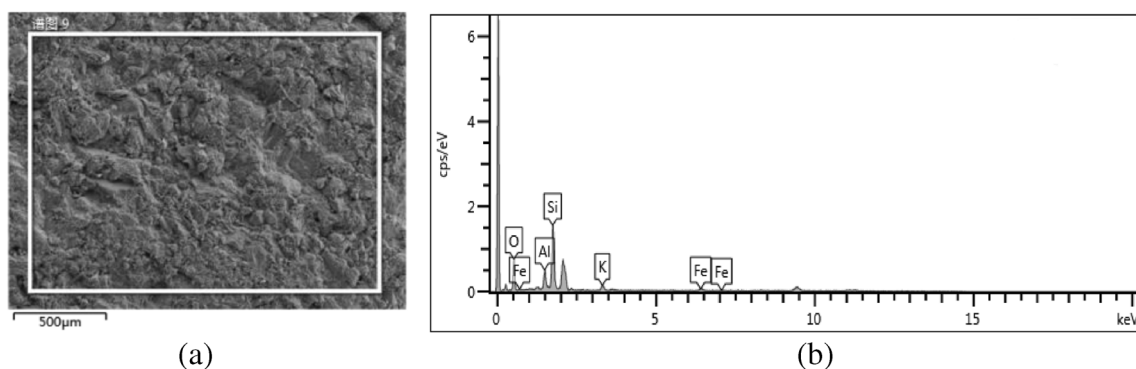

(a)   (b)

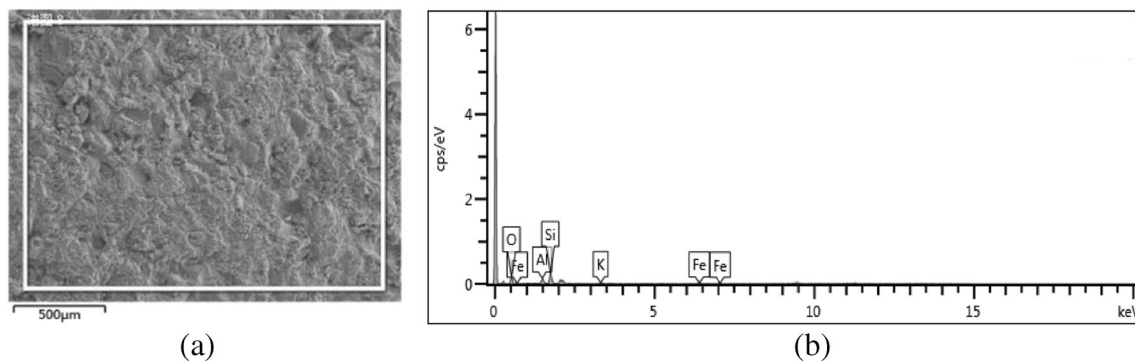**Fig. 7** Energy spectrum analysis of sandstone specimens under 0.1 mol/LNa_2SO_4 pH = 3.0

Fig. 8 Energy spectrum analysis of sandstone specimens under 0.1mol/LNaHCO$_3$ (pH = 3.0)

see a change in their pH balance. This indicated that the acidic Na$_2$SO$_4$ (pH = 3.0) solution aggravated the FT damage and degradation in the internal microstructure of sandstone. That being said, this inhibiting effect disappeared when the samples were immersed in the NaOH (pH = 12.0) solution after 100 FT cycles.

As shown in Figs. 7, 8, 9, 10, and 11, different chemical compositions had varying effects on the damage degree on the internal microstructure of sandstone under the combined effects of chemical solutions and FT cycle. The particle size, grinding, and roundness of the mineral grains in indented rock samples decreased to variable extents when the rocks are immersed in Na$_2$SO$_4$ (pH = 3.0) and NaHCO$_3$ (pH = 3.0) solutions after 100 FT cycles. It was found that their structures also became looser. In addition, the cement between mineral grains composed of CaCO$_3$ began corrosion, and other mineral elements were found to be either significantly scarcer or to have simply disappeared. However, the degree of the internal microstructure of sandstone submerged in the Na$_2$SO$_4$ (pH = 3.0) solution was greater than the sandstone in the NaHCO$_3$ (pH = 3.0) solution. Meanwhile, the results of EDS testing indicated that the basic elements in the Na$_2$SO$_4$ (pH = 3.0) solution were diminished compared to the NaHCO$_3$ (pH = 3.0) solution, while the sandstone submerged in distilled water (pH = 7.0) exhibited fewer basic elements than that for the samples exposed to the Na$_2$SO$_4$ (pH = 7.0) solution. This indicated that Na$_2$SO$_4$ solutions aggravated the FT damage of sandstone, taken from a mesoscopic view.

Analysis of damage variable mechanisms

The sandstone samples used in the study's tests were identified as medium and fine calcareous quartz sandstones via professional mineral appraisal. They were composed primarily of quartz, feldspar (e.g., potassium feldspar, sodium feldspar, and calcium feldspar), small amounts of mica (i.e., biotite and white mica), and a small number of debris and metal minerals. Cementation in the samples was identified as porous cement composed primarily of carbonate. Specifically, the sandstone's quartz was identified as SiO$_2$, an alkaline oxide. The potassium feldspar (or potash feldspar), sodium feldspar, and calcium feldspar were identified as KAlSi$_3$O$_8$, NaAlSi$_3$O$_8$, and CaAl$_2$Si$_3$O$_8$, respectively. The mica was identified as KAl$_3$Si$_3$O$_{10}$(OH)$_2$, and the formula for the main composition of carbonate cement was CaCO$_3$. In addition, the main formulae of the other minerals in the sandstone are K$_2$O, MgO, Na$_2$O, and CaO, respectively.

Chemical corrosion mechanisms

Complex physical and chemical reactions occur when sandstone is immersed in a chemical solution. The physical interaction between water and rock results primarily in the dissolution of the sandstone's minerals in a chemical solution. The primary effect of this upon the sandstone is a general weakening and a reduction in friction force. The chemical interactions between water and rock are composed primarily of the
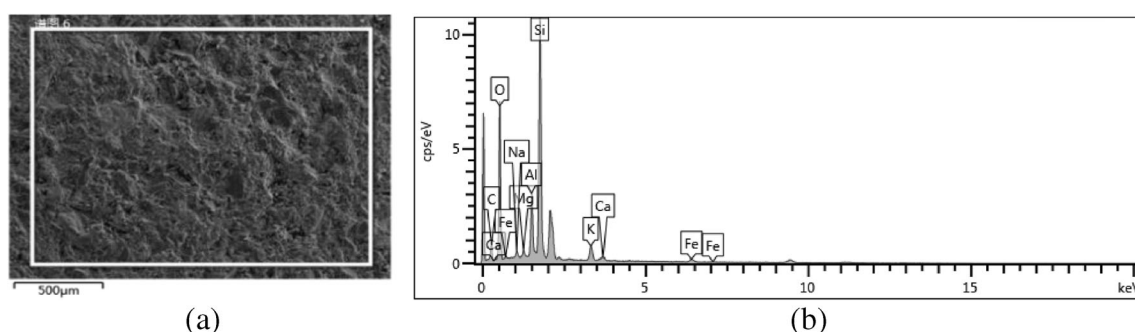

Fig. 9 Energy spectrum analysis of sandstone specimens under 0.1 mol/L NaOH (pH=12.0)
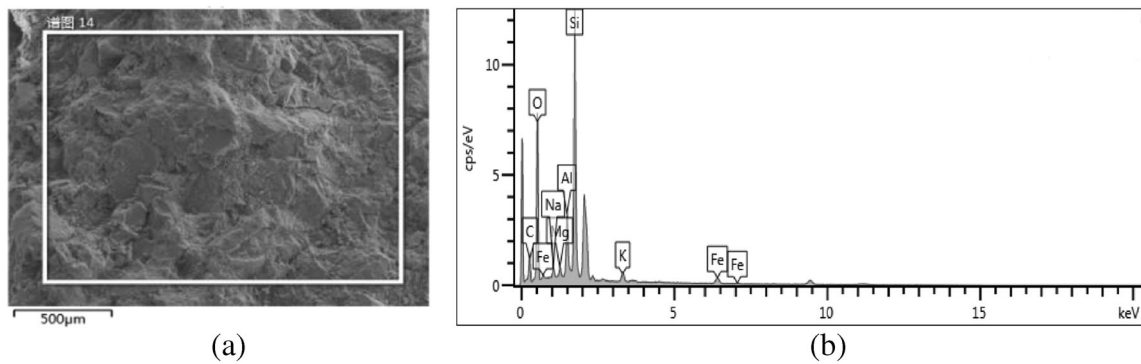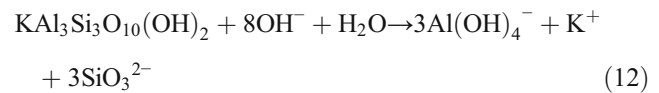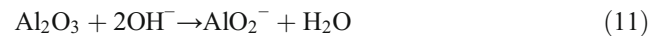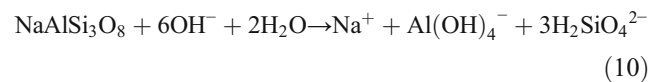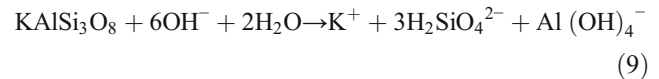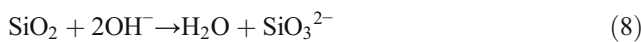
Fig. 10 Energy spectrum analysis of sandstone specimens under natural state

corrosion that occurs in the rock's minerals and chemical solutions. The primary effect of this interaction is an alteration in the particle size of the minerals and their components and an alteration in the rock's pore structure that results in the softening and weakening of the rock. These effects degrade the physical and mechanical characteristics of sandstone to varying degrees, and alterations in the microstructure of rock are simultaneous and concurrently influence each other.

The primary reactions between water and rock, when the samples were immersed in distilled water (pH = 7.0), were shown as the following:

$$MgO + H_2O \rightarrow Mg(OH)_2 \tag{3}$$

$$Na_2O + H_2O \rightarrow 2Na^+ + 2OH^- \tag{4}$$

$$K_2O + H_2O \rightarrow 2K^+ + 2OH^- \tag{5}$$

$$CaO + H_2O \rightarrow Ca(OH)_2 \tag{6}$$

$$SiO_2 + 2H_2O \rightarrow H_4SiO_2 \tag{7}$$

The primary chemical reactions that occurred between the sandstone and 0.1 mol/L NaOH (pH = 12.0) solutions, mutually exclusive with chemical reactions (3) to (7) mentioned previously, were shown as the following:

$$SiO_2 + 2OH^- \rightarrow H_2O + SiO_3^{2-} \tag{8}$$

$$KAlSi_3O_8 + 6OH^- + 2H_2O \rightarrow K^+ + 3H_2SiO_4^{2-} + Al(OH)_4^- \tag{9}$$

$$NaAlSi_3O_8 + 6OH^- + 2H_2O \rightarrow Na^+ + Al(OH)_4^- + 3H_2SiO_4^{2-} \tag{10}$$

$$Al_2O_3 + 2OH^- \rightarrow AlO_2^- + H_2O \tag{11}$$

$$KAl_3Si_3O_{10}(OH)_2 + 8OH^- + H_2O \rightarrow 3Al(OH)_4^- + K^+ + 3SiO_3^{2-} \tag{12}$$

The primary chemical reactions occurred between the sandstone and 0.1 mol/L Na_2SO_4 (pH = 3.0) solution, mutually exclusive with chemical reactions (3) to (7) mentioned previously, were shown as the following:
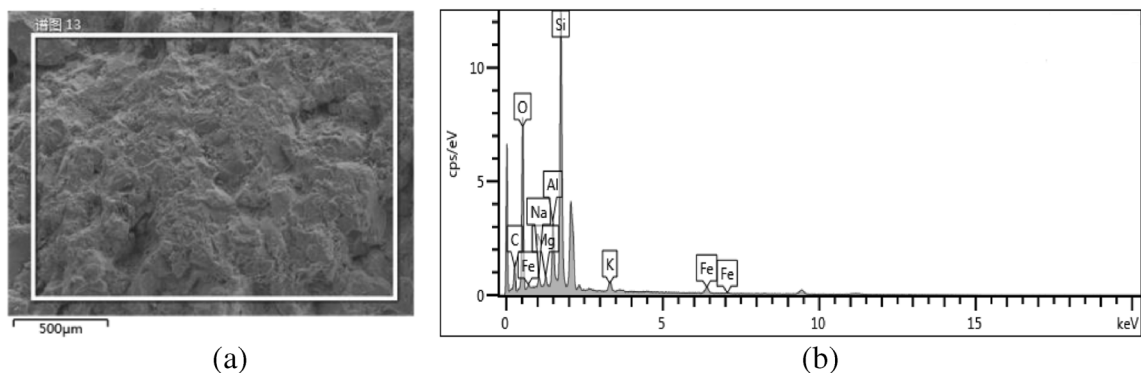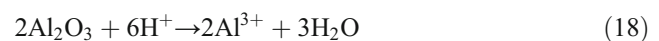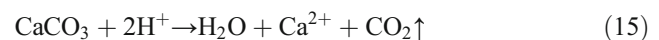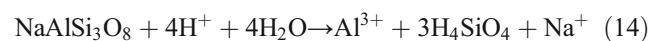
$$KAlSi_3O_8 + 4H^+ + 4H_2O \rightarrow Al^{3+} + 3H_4SiO_4 + K^+ \tag{13}$$

$$NaAlSi_3O_8 + 4H^+ + 4H_2O \rightarrow Al^{3+} + 3H_4SiO_4 + Na^+ \tag{14}$$

$$CaCO_3 + 2H^+ \rightarrow H_2O + Ca^{2+} + CO_2\uparrow \tag{15}$$

$$Na_2O + 2H^+ \rightarrow 2Na^+ + H_2O \tag{16}$$

$$MgO + 2H^+ \rightarrow 2Mg^{2+} + H_2O \tag{17}$$

$$2Al_2O_3 + 6H^+ \rightarrow 2Al^{3+} + 3H_2O \tag{18}$$

$$CaO + 2H^+ \rightarrow 2Ca^{2+} + H_2O \tag{19}$$

$$K_2O + 2H^+ \rightarrow 2K^+ + H_2O \tag{20}$$

Fig. 11 Energy spectrum analysis of sandstone specimens under distilled water pH = 7.0

$$2Fe_2O_3 + 6H^+ \rightarrow 2Fe^{3+} + 3H_2O \qquad (21)$$

$$KAl_3Si_3O_{10}(OH)_2 + 10H^+ \rightarrow K^+ + 3H_4SiO_4 + 3Al^{3+} \quad (22)$$

$$CaMg(CO_3)_2 + 4H^+ \rightarrow Ca^{2+} + Mg^{2+} + H_2O + CO_2\uparrow \quad (23)$$
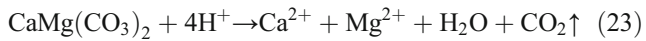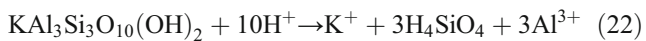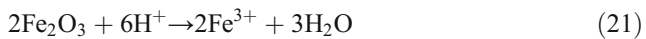
In addition to the chemical reactions listed previously, dissolution and hydrolytic actions between water and rock were also observed. Specifically, the hydrolytic action occurred among the K^+, Ca^{2+}, Na^+, and Mg^{2+} of the rock's mineral and the OH^- ions in the solutions. This reaction resulted in the original minerals dissolving and forming new minerals. In addition, the observed dissolution action caused the minerals in the sandstone to dissolve and disappear completely, additionally increasing the porosity of the rock.

The chemical reactions (3) to (7) previously mentioned were only observed when the sandstone was immersed in 0.1 mol/L Na_2SO_4 (pH = 7.0) solution. No violent chemical reactions occurred between the water and rock products that were poorly soluble in water (e.g., H_4SiO_4, $Ca(OH)_2$, and $Mg(OH)_2$). Regardless, reactions between the two caused the sandstone to become loose, exhibiting a kind of rebuilding effect on the samples' original sandstone cracks therein. After the chemical reaction between the sandstone's K_2O and Na_2O with the Na_2SO_4 (pH = 7.0) solution, the K^+ and Na^+ ions of the chemical reactants were migrated out of the sample and into the solutions, causing the chemical damage in the rock indentations to increase. However, little effect was observed on the mechanical characteristics of the sandstone samples due to the negligible levels of K_2O and Na_2O in sandstone.

The chemical reactions between sandstone and the acidic Na_2SO_4 (pH = 3.0) solution were more characterized as being more severe and eliciting greater variation. Most reaction products were in the form of ions that made the sandstone loose and porous. As a result, the mechanical characteristics of sandstone decreased with the time increased when the sample was immersed in the Na_2SO_4 (pH = 3.0) solutions.

At the initial stage of testing, a path of least resistance presented itself for reaction products to fill in the initial pore defects of the sandstone soaked in the NaOH (pH = 12.0) solution. This was not the case for samples exposed to the Na_2SO_4 (pH = 7.0) solution. The degree of degradation in the mechanical characteristics of the samples soaked in the NaOH (pH = 12.0) solution was smaller than that in the Na_2SO_4 (pH = 7.0) solution. However, the sediment gradually increased with continuous chemical corrosion, expanding via the frost heave effect of the FT cycle. However, these interactions caused the porosity of the samples to increase and further promoted the infiltration of chemical solutions into the sandstone. The chemical damage to the sandstone and the degradation degree in mechanical characteristics of sandstone samples in an alkaline environment increased.

The phenomena of the soaking process indicated that chemical reactions between sandstone and acidic Na_2SO_4 (pH = 3.0) solution were more severe than those in the NaHCO$_3$ (pH = 3.0) solution. In addition, "Test apparatus and test method" showed that the dissolution of the ion concentration in NaHCO$_3$ (pH = 3.0) solution was smaller than that in the Na_2SO_4 (pH = 3.0) solution. Therefore, it can be concluded that Na_2SO_4 (pH = 3.0) solutions had a greater effect on the chemical degradation of sandstone than the NaHCO$_3$ (pH = 3.0) solutions.

Damage mechanisms of the combined effects of chemical corrosion and FT cycles

The damage and degradation occurring in rocks for continued exposure to FT cycles are often subject to varying influences, and the processes involved are very complex. The primary factors are the category of rock material, developmental conditions for the primary pore defects in the rock, the moisture content of the rock, its saturation, the number of FT cycles, the range of FT cycle temperature, and the stress state of the rock itself. Meanwhile, rock can also suffer from the influence of a complex chemical environment. Karfakis and Askram (1993) found that the free water in the interior of rock will freeze completely at temperatures of −5 to −20°C. However, the temperature of the completely frozen free water is reduced significantly in the presence of specific chemical solutions. These solutions can alleviate the degree of FT degradation of rock but also make a rock suffer from the effects of chemical corrosion during the processes of FT cycles. The damage degree of the internal microstructure of rock increases, which affects the degradation of the physical and mechanical properties of the rock to varying degrees.

The temperature gradient between the interior and exterior of sandstone caused by freezing or melting in a number of FT cycles exerted internal stresses upon sandstone. The partial internal damage in rock gradually coalesced, the degradation degree in the internal microstructure gradually increased, and lastly, the physical and mechanical characteristics of the sandstone samples gradually deteriorated as a result of this chain of events. To sum up, the damage and degradation accrued from FT in the rock amounted to a kind of low-cycle fatigue damage.

By observing the samples' surfaces, it was found that it became loose following exposure to repeated FT cycles and resulted in peeling. As the number of FT cycles increased, this phenomenon gradually crept into the interior of sandstone, and the rock's degree of looseness and spalling increased as a result. This indicated that the rate of temperature reaction on the surface of the sandstone was greater than that of its interior when the temperature decreased or increased during the FT cycle. In turn, this brought about a temperature gradient between the interior and exterior of the sandstone which generated tensile stress in some surfaces of the rock. Specifically, when the tensile stress generated by the temperature gradient

was greater than the tensile strength of the rock, the cracks would form on the surface of the rock due to the tensile strength of sandstone was generally quite low. The surface of sandstone samples became loose and fragile thereafter, and with this, the mineral particles in the rock gradually began to peel off after repeated exposure to FT cycles. This phenomenon gradually moved to the interior of samples. Damage and failure in rock began at the surface of samples and moved toward the interior through the FT cycle.

The damage inflicted on the interior microstructure of the sandstone gradually increased under repeated FT cycles. Porosity in the sandstone concurrently increased; this enabled the chemical solutions to further infiltrate into the interior of sandstone. This interaction improved exposure between chemical solutions and mineral grains, making the chemical reactions between water and rock more thorough. The reactants gradually dissolving from the sandstone sustained chemical reaction, and the porosity increased from replenishment of the chemical solution. In addition, moisture content also increased, consistent with the increase in porosity. In the process of freezing, the frost heave pressure effect occurred as more free water gradually froze. This process increased the damage and degradation in the sandstone samples. Water-chemical solutions and FT cycles promote each other in the deterioration of rocks while simultaneously affecting the degree to which damage and deterioration occur in sandstone.

Conclusion

Mode-I fractured sandstone soaked in chemical solutions has a marked tendency toward weakening under FT cycles. An increase in the number of FT cycles leads to a gradual increase in damage of sandstone; the pH and chemical composition of chemical solutions have different effects on the deterioration degree from FT in sandstone.

The surface of the sandstone becomes seriously degraded, for example, holes and pitting corrosion increased under the combined effects of chemical corrosion and FT cycle exposure, and gradually increase with the increasing number of FT cycles. The degree of damage in the microstructures on the surface of sandstone gradually increases correspondingly.

The internal morphology of sandstone in the natural state is relatively coarse. Sandstone is characterized by relatively large mineral particle sizes with a relatively dense internal structure. However, many small mineral particles will form in the indented rock under the combined effects of different chemical solutions and FT cycles. Additionally, the edges and corners of the mineral grains found in sandstone will gradually disappear or smoothen, and the roughness of its mineral grains gradually decreases, exhibiting a looser structure in the rock.

Declarations

Conflict of interest The authors declare that they have no known competing financial interests or personal relationships that could have appeared to influence the work reported in this paper.

References

Aoki K, Hibiya K, Yoshida T (1990) Storage of refrigerated liquefied gases in rock caverns: characteristics of rock under very low temperatures. Tunn Undergr Space Technol 5(4):319–325

Atkinson BK, Meredith PG (1981) Stress corrosion cracking of quartz: a note on the influence of chemical environment. Tectonophysics 77:1–11

Bäckström A, Antikainen J, Backers T (2008) Numerical modelling of uniaxial compressive failure of granite with and without saline porewater. Int J Rock Mech Min Sci 45(7):1126–1142

Cao RH, Wang CS, Yao RB, Hu T, Lei DX, Lin H, Zhao YL (2020) Effects of cyclic freeze-thaw treatments on the fracture characteristics of sandstone under different fracture modes: laboratory testing. Theor Appl Fract Mech 109:102738

Chen Y, Cao P, Chen R (2010) Effect of water-rock interaction on the morphology of a rock surface. Int J Rock Mech Min Sci 47:816–822

Chen YL, Wang P, Zhang XW, Du X (2014) Experimental research on mechanical properties of granite in chemical dissolution under freeze-thaw cycles. J Geotech Eng 36(12):2226–2235 (in Chinese)

DelRoa LM, Lopez F, Esteban FJ (2005) Ultrasonic study of alteration processes in granites caused by freezing and thawing. IEEE Ultrason Symp l:415–418

Dieterich JH, Conrad G (1984) Effects of humidity on time and velocity dependent friction in rocks. J Geophys 89:4196–4202

Dunning J, Douglas B, Millar M, McDonald S (1994) The role of the chemical environment in frictional deformation: stress corrosion cracking and comminution. Pageoph 143(1/2/3):151–178

Fang Y, Qiao L, Chen X (2014) Experimental study of freezing-thawing cycles on sandstone in Yungang grottos. Rock Soil Mech 35(9):2433–2442 (in Chinese)

Fang W, Jiang N, Luo XD (2019) Establishment of damage statistical constitutive model of loaded rock and method for determining its parameters under freeze-thaw condition. Cold Reg Sci Technol 160:31–38

Feng XT, Ding WX (2007) Experimental study of limestone microfracturing under a coupled stress, fluid flow and changing chemical environment. Int J Rock Mech Min Sci 44(3):437–448

Feucht LJ, Logan JM (1990) Effects of chemically active solutions on shearing behavior of a sandstone. Tectonophysics 175:159–176

Fukuda M (1974) Rock weathering by freeze-thaw cycles. Low Temp Sci Ser A Phys Sci 32:243–249

Hallet B (1983) The breakdown of rock due to freezing: a theoretical mode. Proceeding of the 4th International Conference on

Permafrost. Fairbanks, Alaska. National Academy Press, Washington, pp 433–438

Han TL, Shi JP, Chen YS, Cao XS (2019) Mechanism damage to mode-i fractured sandstone from chemical solutions and its correlation with strength characteristics. Pure Appl Geophys 176:5027–5049

Inada Y, Yokota K (1984) Some studies of low temperature rock strength. Int J Rock Mech Min Sci Geomech Abstr 21(3):145–153

Jia Y, Bian HB, Xie SY (2017) Burlion N, Shao JF. A numerical study of mechanical behavior of a cement paste under mechanical loading and chemical leaching. Int J Numer Anal Methods Geomech 41(18): 1848-1869.

Karfakis MG, Askram M (1993) Effects of chemical solutions on rock fracturing. Int J Rock Mech Min Sci Geomech Abstr 37(7):1253–1259

Koorosh A, Mehdi H, Morteza S (2020) Effect of freezing temperature and number of freeze-thaw cycles on mode i and mode ii fracture toughness of sandstone. Theor Appl Fract Mech 105:102428

Lajtai EZ, Schmidtke RH, Bielus LP (1987) The effect of water on the time-dependent deformation and fracture of a granite. Int J Rock Mech Min Sci Geomech Abstr 24(4):247–255

Li S, Huo R, Wang B, Ren Z (2018) Experimental study on physicomechanical properties of sandstone under acidic environment. Adv Civ Eng 4:1–15

McGreevy JP (1985) Rock moisture content and frost weathering under natural and experimental conditions: a comparative discussion. Arct Alp Res 17(3):337–346

Nara Y, Morimoto K, Hiroyoshi N (2012) Influence of relative humidity on fracture toughness of rock: implications for subcritical crack growth. Int J Solids Struct 49:2471–2481

Négrel P, Millot R, Roy S (2010) Lead isotopes in groundwater as an indicator of water-rock interaction (Masheshwaram catchment, Andhra Pradesh, India). Chem Geol 274(3):136–148

Norikazu M (1990) Mechanisms of rock breakdown by frost action: an experimental approach. Cold Reg Sci Technol 17(3):253–270

Reinhardt HW, Mielich O, Reinhardt HW (2014) Fracture toughness of alkali-sensitive rocks in alkaline solution. Int J Rock Mech Min Sci 70:552–558

Tan XJ, Chen WZ, Yang JP (2011) Laboratory investigations on the mechanical properties degradation of granite under freeze-thaw cycles. Cold Reg Sci Technol 68:130–138

Terzaghi K (1943) Theoretical soil mechanics. John Wiley & Sons, New York

The Professional Standard Compilation Group of People's Republic of China (2007) DL/T5368-2007 Specifications for rock tests in water conservancy and hydroelectric engineering. China Water Power Press, Beijing (in Chinese)

Wu XD (2013) Experimental study on the time-dependent behaviour of Xiangjiaba sandstone. Appl Mech Mater 256-259:174–178

Yamabe T, Neaupane KM (2001) Determination of some the thermo-mechanical properties of Sirahama sandstone under subzero temperature conditions. Int J Rock Mech Min Sci 38(7):1029–1034

Yavuz H, Altindag R, Sarac S (2006) Estimating the index properties of deteriorated carbonate rocks due to freeze-thaw and thermal shock weathering. Int J Rock Mech Min Sci 43(5):767–775

Zeng T, Shao JF, Xu WY (2015) A micromechanical model for the elastic-plastic behavior of porous rocks. Comput Geotech 70:130–137

Zhang R, Ai T, Ren L, Li G (2019) Failure characterization of three typical coal-bearing formation rocks using acoustic emission monitoring and X-ray computed tomography techniques. Rock Mech Rock Eng 52:1945–1958

Zhou ZW, Ma W, Zhang SJ, Mu YH, Li GY (2018) Effect of freeze-thaw cycles in mechanical behaviors of frozen loess. Cold Reg Sci Technol 146:9–18